1

Modeling of AC Drives and Power Converter

Building mathematical models of *AC* drives and power converters is the first step towards the design and implementation of control systems. This chapter presents the mathematical models of machine drives and power converters in a uniform way that firstly uses space vector description of the physical variables such as voltage, current and flux, and secondly converts the space vector based model to various reference frames. From Sections 1.1 to 1.4, the Permanent Magnetic Synchronous Machine (PMSM) will be used as an example to illustrate in detail how its dynamic model is established. In Section 1.5, the dynamic model for an induction machine is obtained by following the same thought process used for the PMSM. Section 1.6 derives the dynamic model for a 2-level grid connected voltage source converter, also using the same approaches as electrical drives. In the Summary section 1.7, characteristics of dynamic models are highlighted for future applications.

1.1 Space Phasor Representation

The analysis of a three phase system could be significantly simplified by adopting vector based approaches. Here, the concept of space vector will be introduced first before deriving a model of a PMSM. To simplify the analysis, a 2-pole machine with balanced three phase windings is assumed.

1.1.1 Space Vector for Magnetic Motive Force

Figure 1.1 shows the cross section of stator windings for a 2-pole machine. By Ampere's law, a magnetic motive force (MMF) will be generated when current is flowing in the windings. The peak of magnetic motive force produced by each phase will align with their own magnetic field and is separated by 120° from each other. Here, it is assumed that phase current has a frequency ω, initial angle ϕ_0 and amplitude I_s. When each of the three phase windings is provided with balanced three phase currents, where

$$i_a(t) = I_s \cos(\omega t + \phi_0) \tag{1.1}$$

$$i_b(t) = I_s \cos(\omega t + \phi_0 - 2\pi/3) \tag{1.2}$$

$$i_c(t) = I_s \cos(\omega t + \phi_0 - 4\pi/3). \tag{1.3}$$

PID and Predictive Control of Electrical Drives and Power Converters using MATLAB®/Simulink®, First Edition.
Liuping Wang, Shan Chai, Dae Yoo, Lu Gan and Ki Ng.

Companion Website: www.wiley.com/go/wang/pid

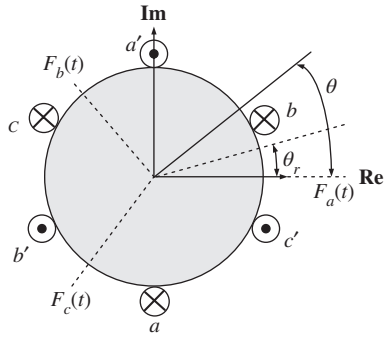

Figure 1.1 Cross section of stator winding. ⊗ and ⊙ denote the cross sections of the wires, $F_a(t)$, $F_b(t)$ and $F_c(t)$ are the peaks of magnetic motive forces for the three phase currents, θ_r is the position of the rotor and θ is an arbitrary position.

each phase current will produce a sinusoidal distributed MMF whose peak aligns with their respective magnetic axis for each phase, which are

$$F_a(t) = N_s i_a(t) = F_m \cos(\omega t + \phi_0) \tag{1.4}$$

$$F_b(t) = N_s i_b(t) = F_m \cos(\omega t + \phi_0 - 2\pi/3) \tag{1.5}$$

$$F_c(t) = N_s i_c(t) = F_m \cos(\omega t + \phi_0 - 4\pi/3), \tag{1.6}$$

where $F_m = N_s I_s$ is the magnitude of the peak MMF, N_s is a constant related to the number of coil turns and winding factor and I_s is the amplitude of the phase current.

At a certain position θ, referred to the magnetic axis of phase **a-a'** in Figure 1.1, the magnetic motive forces contributed from each phase winding are

$$F_a(t)^\theta = F_a(t)\cos(0 - \theta) \tag{1.7}$$

$$F_b(t)^\theta = F_b(t)\cos(2\pi/3 - \theta) \tag{1.8}$$

$$F_c(t)^\theta = F_c(t)\cos(4\pi/3 - \theta), \tag{1.9}$$

which are functions of θ. Therefore, the resultant total MMF at the position θ is the summation of Equations (1.7)–(1.9), which gives

$$F(t)^\theta = F_a(t)\cos(-\theta) + F_b(t)\cos(2\pi/3 - \theta) + F_c(t)\cos(4\pi/3 - \theta). \tag{1.10}$$

Note that

$$\cos(-\theta) = \mathbf{Re}\{e^{-j\theta}\}; \quad e^{-j\theta} = \cos(\theta) - j\sin(\theta).$$

Equation (1.10) can also be represented by

$$\begin{aligned} F(t)^\theta &= \mathbf{Re}\{F_a(t)e^{-j\theta} + F_b(t)e^{-j(\theta-2\pi/3)} + F_c(t)e^{-j(\theta-4\pi/3)}\} \\ &= \frac{3}{2}\mathbf{Re}\left\{\frac{2}{3}\left(F_a(t) + F_b(t)e^{j\frac{2\pi}{3}} + F_c(t)e^{j\frac{4\pi}{3}}\right)e^{-j\theta}\right\}. \end{aligned} \tag{1.11}$$

Based on the calculation of the total MMF at the position θ, the space vector of the three-phase peak MMF is defined by

$$\vec{F}(t) = \frac{2}{3}\left(F_a(t) + F_b(t)e^{j\frac{2\pi}{3}} + F_c(t)e^{j\frac{4\pi}{3}}\right). \tag{1.12}$$

For notational simplicity, the rest of this chapter will use the notation $\overrightarrow{\{.\}}$ to denote a space vector. With this definition, the total MMF at the position θ is expressed as

$$F(t)^{\theta} = \frac{3}{2}\mathbf{Re}\left\{\overrightarrow{F}(t)e^{-j\theta}\right\}. \tag{1.13}$$

Furthermore, it can be verified that by substituting (1.4)–(1.6) into (1.12), the space vector of the three-phase peak MMF $\overrightarrow{F}(t)$ has the following compact expression:

$$\begin{aligned}\overrightarrow{F}(t) &= \frac{2}{3}\left(F_a(t) + F_b(t)e^{j\frac{2\pi}{3}} + F_c(t)e^{j\frac{4\pi}{3}}\right)\\ &= \frac{2}{3}F_m\left(\cos(\omega t + \phi_0) + \cos(\omega t + \phi_0 - 2\pi/3)e^{j\frac{2\pi}{3}} + \cos(\omega t + \phi_0 - 4\pi/3)e^{j\frac{4\pi}{3}}\right)\\ &= F_m e^{j(\omega t+\phi_0)}.\end{aligned} \tag{1.14}$$

In the derivation of (1.14), the following equalities are used:

$$\cos(\alpha) = \frac{1}{2}(e^{j\alpha} + e^{-j\alpha})$$

$$1 + e^{j\frac{4\pi}{3}} + e^{j\frac{8\pi}{3}} = 0.$$

Following the compact expression of $\overrightarrow{F}(t)$ given by (1.14), the total MMF at the position θ is also simply expressed as

$$\begin{aligned}F(t)^{\theta} &= \frac{3}{2}\mathbf{Re}(\overrightarrow{F}(t)e^{-j\theta})\\ &= \frac{3}{2}F_m\cos(\omega t + \phi_0 - \theta).\end{aligned} \tag{1.15}$$

As shown by (1.14), the space vector $\overrightarrow{F}(t)$ is a rotating vector in the complex plane. As a result, the instantaneous value of $F(t)^{\theta}$ in (1.11) and its equivalent (1.15) can be interpreted as the magnitude of the projection of $\overrightarrow{F}(t)$ on the position θ.

Figure 1.2 gives an example of the vector representation of MMF at $t = 0$ while assuming $\phi_0 = 0$. In this figure, at $t = 0$, the vectors of peak MMF for each phase current are

$$\overrightarrow{F_a} = F_m\cos(0)e^{j0} = F_m$$

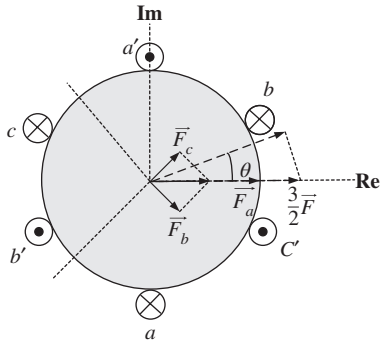

Figure 1.2 Space vector of MMF ($t = 0$ and $\phi_0 = 0$).

$$\overrightarrow{F_b} = F_m \cos\left(-\frac{2\pi}{3}\right) e^{j\frac{2\pi}{3}} = \frac{-1}{2} F_m e^{j\frac{2\pi}{3}}$$
$$\overrightarrow{F_c} = F_m \cos\left(-\frac{4\pi}{3}\right) e^{j\frac{4\pi}{3}} = \frac{-1}{2} F_m e^{j\frac{4\pi}{3}}$$

and the resulting total peak MMF is,

$$\overrightarrow{F} = \frac{2}{3}(\overrightarrow{F_a} + \overrightarrow{F_b} + \overrightarrow{F_c}) = F_m.$$

thus, the total MMF at angle θ is the magnitude of projection $\overrightarrow{F}$ onto angle θ,

$$F(0)^{\theta} = F_m \cos(\theta).$$

1.1.2 Space Vector Representation of Voltage Equation

The use of space vector facilitates the derivation of voltage equation for the PMSM with a compact expression. This derivation is the key to form the dynamic model for current control.

With a similar principle, the space vector for three-phase stator current can be written as

$$\overrightarrow{i_s} = \frac{2}{3}\left(i_a(t) + i_b(t)e^{j\frac{2\pi}{3}} + i_c(t)e^{j\frac{4\pi}{3}}\right) \tag{1.16}$$

$$\overrightarrow{i_s} = I_s e^{j(\omega t + \phi_0)} \tag{1.17}$$

and the space vector of three-phase stator voltage is defined as

$$\overrightarrow{v_s} = \frac{2}{3}\left(v_a(t) + v_b(t)e^{j\frac{2\pi}{3}} + v_c(t)e^{j\frac{4\pi}{3}}\right), \tag{1.18}$$

where $v_a(t)$, $v_b(t)$ and $v_c(t)$ are terminal line-to-neutral voltage for each phase, respectively.

When a surface-mounted PMSM is considered, the space vector of stator flux consists of two parts. One is produced by the stator current while the other is produced by the permanent magnets of the rotor:

$$\overrightarrow{\varphi_s} = L_s \overrightarrow{i_s} + \phi_{mg} e^{j\theta_e}, \tag{1.19}$$

where ϕ_{mg} is the amplitude of the flux induced by the permanent magnets of the rotor in the stator phases and this parameter is assumed constant in the design, θ_e is the electrical angle of the rotor, and L_s is the sum of leakage inductance and mutual inductance.

With the space vector representation of voltage, current and flux, the stator voltage equation in space vector form can be written according to voltage law,

$$\overrightarrow{v_s} = R_s \overrightarrow{i_s} + \frac{d\overrightarrow{\varphi_s}}{dt}, \tag{1.20}$$

where $\overrightarrow{v_s}$ is the space vector of stator voltage, $R_s\overrightarrow{i_s}$ is the voltage drop on the resistors of the stator and $\frac{d\overrightarrow{\varphi_s}}{dt}$ is the induced voltage due to changing of magnetic flux. Taking the derivative of the second term of the flux based on (1.19) gives

$$\frac{d(\phi_{mg}e^{j\theta_e})}{dt} = j\omega_e \phi_{mg} e^{j\theta_e},$$

where $\theta_e(t) = \omega_e t$. Thus, the vector voltage equation of a PMSM is obtained by replacing the flux derivative in (1.20) with the calculated derivative based on (1.19), which leads to

$$\overrightarrow{v_s} = R_s \overrightarrow{i_s} + L_s \frac{d\overrightarrow{i_s}}{dt} + j\omega_e \phi_{mg} e^{j\theta_e}. \tag{1.21}$$

This is the fundamental equation that governs the relationship between the current and voltage of PMSM in a space vector form, based on which the dynamic models will be obtained.

1.2 Model of Surface Mounted PMSM

As seen from the previous sections, the space vectors of three-phase voltages, currents and flux are three rotating vectors in the complex plane. The speed of their rotation depends on the frequency (ω) of the three-phase voltages and currents. In the complex plane, as shown in Figure 1.3, each vector (see the three phase current $\overrightarrow{i_s}$) could be decomposed into a component on real axis (see i_α) and a quadrature component on imaginary axis (see i_β). Such a decomposition could be carried out with respect to different reference frames (see the $d-q$ reference frame). Importantly, control strategies will devised according to the models in the relevant reference frames.

This section presents the two most widely adopted reference frames and their relationships, which are the stationary reference frame (also called $\alpha-\beta$ reference frame) and the synchronous reference frame (also called $d-q$ reference frame). Both reference frames are illustrated in Figure 1.3.

1.2.1 Representation in Stationary Reference ($\alpha-\beta$) Frame

One choice of the reference frame is a stationary reference frame with the real (α) axis aligned with the peak MMF ($F_a(t)$, see Figure 1.1) and the imaginary (β) axis in quadrature (see Figure 1.3).

By projecting the space vectors of voltage and current onto real (α) and imaginary (β) axes, these vectors can be represented by the complex notations,

$$\overrightarrow{v_s} = v_\alpha + jv_\beta \tag{1.22}$$

$$\overrightarrow{i_s} = i_\alpha + ji_\beta. \tag{1.23}$$

Substituting the complex representations (1.22) and (1.23) into the space vector voltage equation (1.21), and equating their real and imaginary parts in both sides, respectively, gives the model of PMSM in the $\alpha-\beta$ reference frame,

$$v_\alpha = R_s i_\alpha + L_s \frac{di_\alpha}{dt} - \omega_e(t)\phi_{mg}\sin\theta_e \tag{1.24}$$

$$v_\beta = R_s i_\beta + L_s \frac{di_\beta}{dt} + \omega_e(t)\phi_{mg}\cos\theta_e. \tag{1.25}$$

This model of PMSM will be used in the Chapter 7 for a current controller design in the $\alpha-\beta$ reference frame.

One might ask what is the relationship between the current and voltage variables in the $\alpha-\beta$ reference frame and the original three phase variables. This unique relationship is given by the Clarke

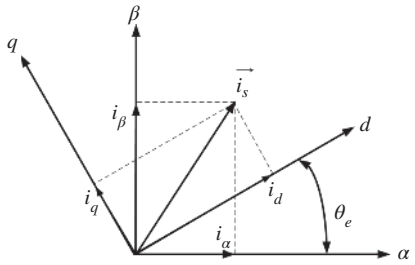

Figure 1.3 Illustration of stationary reference frame and synchronous reference frame. θ_e is the electrical angle of the rotor. Current space vector is projected to two reference frames.

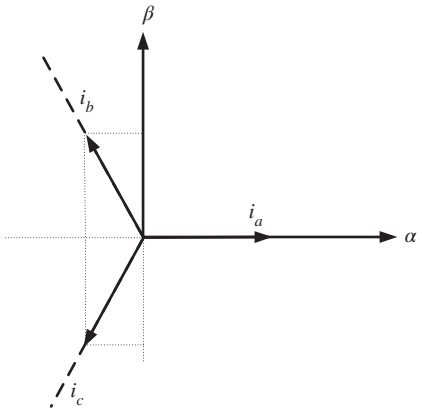

Figure 1.4 Illustration of Clarke transformation of current.

transformation. Taking the three phase currents as an example, the transformation of three phase variables to their components in the $\alpha - \beta$ reference frame is achieved by Clarke transformation, where

$$\begin{bmatrix} i_\alpha \\ i_\beta \\ i_0 \end{bmatrix} = \frac{2}{3}\begin{bmatrix} 1 & -\frac{1}{2} & -\frac{1}{2} \\ 0 & \frac{\sqrt{3}}{2} & -\frac{\sqrt{3}}{2} \\ \frac{1}{2} & \frac{1}{2} & \frac{1}{2} \end{bmatrix}\begin{bmatrix} i_a \\ i_b \\ i_c \end{bmatrix}. \tag{1.26}$$

As shown in Figure 1.4, the transformation matrix is obtained by projecting i_a, i_b and i_c on α and β axes, respectively. Here, it is seen that the α axis is aligned with the direction of i_a current which is also the direction of the peak MMF $F_a(t)$ (see Figure 1.1). The coefficient $\frac{2}{3}$ here is to guarantee the energy conservation. In addition, i_0 represents the zero sequence component of three phase current and is zero for balanced three phase currents. Conversely, the inverse Clarke transformation is defined as

$$\begin{bmatrix} i_a \\ i_b \\ i_c \end{bmatrix} = \begin{bmatrix} 1 & 0 & 1 \\ -\frac{1}{2} & \frac{\sqrt{3}}{2} & 1 \\ -\frac{1}{2} & -\frac{\sqrt{3}}{2} & 1 \end{bmatrix}\begin{bmatrix} i_\alpha \\ i_\beta \\ i_0 \end{bmatrix}. \tag{1.27}$$

It is easy to show that

$$\frac{2}{3}\begin{bmatrix} 1 & -\frac{1}{2} & -\frac{1}{2} \\ 0 & \frac{\sqrt{3}}{2} & -\frac{\sqrt{3}}{2} \\ \frac{1}{2} & \frac{1}{2} & \frac{1}{2} \end{bmatrix}\begin{bmatrix} 1 & 0 & 1 \\ -\frac{1}{2} & \frac{\sqrt{3}}{2} & 1 \\ -\frac{1}{2} & -\frac{\sqrt{3}}{2} & 1 \end{bmatrix} = \begin{bmatrix} 1 & 0 & 0 \\ 0 & 1 & 0 \\ 0 & 0 & 1 \end{bmatrix}.$$

The current and voltage variables in the $\alpha - \beta$ reference frame are all sinusoidal in nature because they are directly related to their original three phase current and voltage variables (see the Clarke transformation (1.26)).

1.2.2 Representation in Synchronous Reference ($d-q$) Frame

Another reference frame is the $d-q$ reference frame, where the direct axis (d) is always aligned with rotating flux produced by the permanent magnets of the rotor, and the q axis is in quadrature. Because the rotor runs the same speed as the supplying frequency at steady-state, it is also called the synchronous frame for PMSM.

To change the reference frame to the $d-q$ reference frame, as shown in Figure 1.3, it is equivalent to rotating the space vector in $\alpha-\beta$ reference frame clockwise by θ_e. Mathematically, this rotation of space vectors is translated into multiplication by the factor $e^{-j\theta_e}$, which leads to a set of new space vectors, for example, voltage space vector $\vec{v}_s'$, current space vector $\vec{i}_s'$. By projecting these transformed space vectors into the real and imaginary axes, the current and voltage variables in the $d-q$ reference frame are formed. That is,

$$\vec{v}_s' = \vec{v}_s e^{-j\theta_e} = v_d + jv_q \tag{1.28}$$

$$\vec{i}_s' = \vec{i}_s e^{-j\theta_e} = i_d + ji_q \tag{1.29}$$

where $\vec{v}_s'$ and $\vec{i}_s'$ denote the space vectors referred to synchronous $d-q$ reference frame.

Multiplying the the original space vector voltage equation (1.21) by $e^{-j\theta_e}$ leads to the following equation:

$$\vec{v}_s e^{-j\theta_e} = R_s \vec{i}_s e^{-j\theta_e} + L_s \frac{d\vec{i}_s}{dt} e^{-j\theta_e} + j\omega_e \phi_{mg}. \tag{1.30}$$

Noting that

$$\vec{i}_s' = \vec{i}_s e^{-j\theta_e}$$

and by taking derivative on both sides of this equality, it can be shown that

$$\frac{d\vec{i}_s}{dt} e^{-j\theta_e} = \frac{d\vec{i}_s'}{dt} + j\omega_e \vec{i}_s'. \tag{1.31}$$

Therefore, from (1.30), together with (1.31), the voltage equation in terms of the space vectors $\vec{v}_s'$ and $\vec{i}_s'$ has the following form:

$$\vec{v}_s' = R_s \vec{i}_s' + L_s \frac{d\vec{i}_s'}{dt} + j\omega_e L_s \vec{i}_s' + j\omega_e \phi_{mg}. \tag{1.32}$$

This is the fundamental equation that governs the relationship between the voltage and current variables in space vector form that leads to the dynamic model in the $d-q$ reference frame.

Now, substituting (1.28) and (1.29) into (1.32), and because the real and imaginary components from the left-hand side are equal to the corresponding components in their right-hand side, it can be shown that the $d-q$ model of PMSM is,

$$v_d = R_s i_d + L_s \frac{di_d}{dt} - \omega_e L_s i_q \tag{1.33}$$

$$v_q = R_s i_q + L_s \frac{di_q}{dt} + \omega_e L_s i_d + \omega_e \phi_{mg}, \tag{1.34}$$

where (1.33) is obtained with the components from the real part whilst (1.34) is from the imaginary part.

There is a unique relationship between the variables in the $\alpha-\beta$ reference frame and those in the $d-q$ reference frame. The transformation of real and imaginary components in $\alpha-\beta$ frame to its counterparts

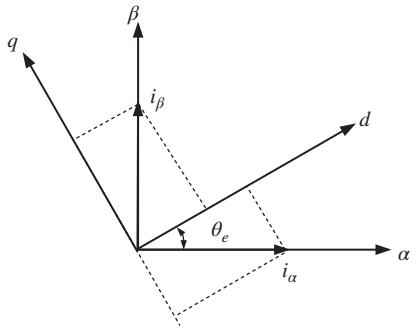

Figure 1.5 Illustration of Park transformation of current from $d-q$ reference frame to $\alpha-\beta$ reference frame.

in the rotating $d-q$ reference frame is achieved by the so called Park transformation, as shown in Figure 1.5, which leads to the current and voltage relations in the two reference frames:

$$\begin{bmatrix} v_d \\ v_q \end{bmatrix} = \begin{bmatrix} \cos\theta_e & \sin\theta_e \\ -\sin\theta_e & \cos\theta_e \end{bmatrix} \begin{bmatrix} v_\alpha \\ v_\beta \end{bmatrix} \tag{1.35}$$

$$\begin{bmatrix} i_d \\ i_q \end{bmatrix} = \begin{bmatrix} \cos\theta_e & \sin\theta_e \\ -\sin\theta_e & \cos\theta_e \end{bmatrix} \begin{bmatrix} i_\alpha \\ i_\beta \end{bmatrix}, \tag{1.36}$$

where θ_e is the angle between the two reference frames and also the electrical angle of the rotor.

Conversely, the inverse Park transformation is defined as

$$\begin{bmatrix} v_\alpha \\ v_\beta \end{bmatrix} = \begin{bmatrix} \cos\theta_e & -\sin\theta_e \\ \sin\theta_e & \cos\theta_e \end{bmatrix} \begin{bmatrix} v_d \\ v_q \end{bmatrix} \tag{1.37}$$

$$\begin{bmatrix} i_\alpha \\ i_\beta \end{bmatrix} = \begin{bmatrix} \cos\theta_e & -\sin\theta_e \\ \sin\theta_e & \cos\theta_e \end{bmatrix} \begin{bmatrix} i_d \\ i_q \end{bmatrix}. \tag{1.38}$$

Combining Clarke transformation (1.26) with Park transformation (1.36) gives the Park-Clarke transformation from three-phase values to their representations in the $d-q$ reference frame:

$$\begin{bmatrix} i_d \\ i_q \end{bmatrix} = \frac{2}{3} \begin{bmatrix} \cos\theta_e & \cos\left(\theta_e - \frac{2\pi}{3}\right) & \cos\left(\theta_e - \frac{4\pi}{3}\right) \\ -\sin\theta_e & -\sin\left(\theta_e - \frac{2\pi}{3}\right) & -\sin\left(\theta_e - \frac{4\pi}{3}\right) \end{bmatrix} \begin{bmatrix} i_a \\ i_b \\ i_c \end{bmatrix}. \tag{1.39}$$

The amazing fact about the mathematical model (see (1.33) and (1.34)) in the $d-q$ reference frame is that the current and voltage variables are no longer sinusoidal signals, instead, they are *DC* signals. In other words, because of this, in the design of a control system, the reference signals to the closed-loop system could be constants or step signals, which explains why PI controllers are widely used for this class of systems.

1.2.3 Electromagnetic Torque

For the surface mounted PMSM, the $d-q$ axis inductance is equal to each other due to the uniform air-gap, that is

$$L_d = L_q = L_s$$

and thus the stator flux in $\alpha - \beta$ reference frame is as in Equation (1.19). Similarly, the stator flux can also be represented in the $d - q$ frame by rotating the flux vector clockwise by θ_e, leading to

$$\vec{\varphi}_s{}' = \vec{\varphi}_s e^{-j\theta_e} = L_s \vec{i}_s{}' + \phi_{mg} \tag{1.40}$$

and its real and imaginary parts are

$$\varphi_d = L_s i_d + \phi_{mg} \tag{1.41}$$

$$\varphi_q = L_s i_q \tag{1.42}$$

respectively, where the flux (ϕ_{mg}) induced by the permanent magnets of the rotor is aligned with rotor and its q-axis component is zero.

The electromagnetic torque is computed as the cross product[1] of the space vector of the stator flux with stator current in the $\alpha - \beta$ reference frame as

$$T_e = \frac{3}{2} Z_p \vec{\varphi}_s \otimes \vec{i}_s \tag{1.43}$$

or equivalently, in the $d - q$ reference frame as,

$$T_e = \frac{3}{2} Z_p \vec{\varphi}_s{}' \otimes \vec{i}_s{}', \tag{1.44}$$

where Z_p is the number of pole pairs. The cross product is calculated using two three dimensional vectors $[\varphi_d, \varphi_q, 0]$ and $[i_d, i_q, 0]$ and the result is the vector $[0, 0, \varphi_d i_q - \varphi_q i_d]$. Hence,

$$T_e = \frac{3}{2} Z_p (\varphi_d i_q - \varphi_q i_d). \tag{1.45}$$

By substituting Equations (1.41) and (1.42) into (1.45), we obtain

$$T_e = \frac{3}{2} Z_p \phi_{mg} i_q. \tag{1.46}$$

With the flux of permanent magnet assumed to be a constant, the electromagnetic torque can be controlled through varying the q-axis component of stator currents. Therefore, with the electrical model of PMSM in $d - q$ reference frame, the control of PMSM is analogous to the principle of controlling *DC* motors.

However, if one were to use the electrical model in the $\alpha - \beta$ reference frame to compute the electromagnetic torque T_e, the matter would be more complicated. In this case, the space vector of the flux has the relationship with the currents in the $\alpha - \beta$ reference frame:

$$\vec{\varphi}_s = L_s \vec{i}_s + \phi_{mg} e^{j\theta_e} \tag{1.47}$$

$$= L_s i_\alpha + \phi_{mg} \cos\theta_e + j (L_s i_\beta + \phi_{mg} \sin\theta_e). \tag{1.48}$$

This leads to the expression of the electromagnetic torque T_e via the cross product of $\vec{\varphi}_s \otimes \vec{i}_s$ that has the following form:

$$T_e = \frac{3}{2} Z_p [(L_s i_\alpha + \phi_{mg} \cos\theta_e) i_\beta - (L_s i_\beta + \phi_{mg} \sin\theta_e) i_\alpha]. \tag{1.49}$$

One could easily compute the torque T_e from (1.49), when the i_α and i_β currents are given. However, in reverse, it would be difficult to determine the trajectories of i_α and i_β if a desired electromagnetic torque

[1] The cross product of two vectors $\vec{a}$ and $\vec{b}$ is the vector $\vec{c} = \vec{a} \otimes \vec{b}$. Letting $\vec{a} = [a_1, a_2, a_3]$ and $\vec{b} = [b_1, b_2, b_3]$, the vector $\vec{c} = [c_1, c_2, c_3]$ has the components: $c_1 = a_2 b_3 - a_3 b_2$, $c_2 = a_3 b_1 - a_1 b_2$ and $c_3 = a_1 b_2 - a_2 b_1$ (see Kreyszig (2010)).

T_e were given, which is what is required in the control of the electromagnetic torque. This explains why in the control strategies chosen for the later chapters, the mathematical model in the $d-q$ reference frame is predominately used for the reason that there is a simple relation between the electromagnetic torque T_e and the i_q current (see (1.46)).

It is worthwhile to emphasize that in the context of controlling a PMSM drive, if the model used for the control system design is based on the $\alpha-\beta$ reference frame, then the manipulated variables are the voltage variables v_α and v_β. Similarly, if the model in the $d-q$ reference frame is used in the design, then the manipulated variables are the voltage variables v_d and v_q. However, in the implementation of the control law, the control signals v_d and v_q will be converted to v_α and v_β signals using the inverse Park Transform, then to three phase voltage signals v_a, v_b and v_c that will be realized using a voltage source inverter typically consisting of a *DC* power supply and several semiconductor switches (see Chapter 2). The same control law implementation procedure applies to other *AC* machine drives and power converters.

1.3 Model of Interior Magnets PMSM

The main difference between an interior magnets PMSM and a surface mounted motor is that the salience due to the rotor magnets results in a non-uniform air-gap flux. The derivation of its $d-q$ model is very similar to the surface mounted case and is briefly introduced here. The vector voltage equations are the same as those in (1.20) and (1.32) and presented here again for convenience,

$$\vec{v_s} = R_s\vec{i_s} + \frac{d\vec{\varphi_s}}{dt} \tag{1.50}$$

$$\vec{v_s}' = R_s\vec{i_s}' + \frac{d\vec{\varphi_s}'}{dt} + j\omega_e\vec{\varphi_s}'. \tag{1.51}$$

In contrast to a surface mounted PMSM, the stator flux due to the salience of the interior magnets needs to be modeled in the $d-q$ reference frame with different inductances in the $d-q$ axes,

$$\vec{\varphi_s}' = \varphi_d + j\varphi_q, \tag{1.52}$$

where

$$\varphi_d = L_d i_d + \phi_{mg} \tag{1.53}$$

$$\varphi_q = L_q i_q. \tag{1.54}$$

Here the quadrature axis stator inductance L_q is usually smaller than the direct axis inductance L_d for an interior magnets PMSM. Therefore, substituting (1.52), (1.53) and (1.54) into (1.51) yields the $d-q$ model for interior magnets PMSM,

$$v_d = R_s i_d + L_d\frac{di_d}{dt} - \omega_e L_q i_q \tag{1.55}$$

$$v_q = R_s i_q + L_q\frac{di_q}{dt} + \omega_e L_d i_d + \omega_e\phi_{mg}. \tag{1.56}$$

It is apparent that the model of interior PMSM is equivalent to the surface mounted case if $L_d = L_q = L_s$. For the interior magnets PMSM, the nonlinearity of torque is mainly due to the salience of the rotor, which causes the non-uniformity of air-gap.

Its electromagnetic torque is obtained by substituting (1.53), (1.54) into (1.45):

$$T_e = \frac{3}{2}Z_p(\phi_{mg}i_q + (L_d - L_q)i_d i_q). \tag{1.57}$$

In comparison with torque equation (1.46) of a surface mounted machine, the extra component $\frac{3}{2}Z_p(L_d - L_q)i_d i_q$ is the reluctance torque due to the saliency.

1.3.1 Complete Model of PMSM

For the PMSM with multiple pair of poles, the electrical speed relates to the mechanical speed by

$$\omega_e = Z_p \omega_m \tag{1.58}$$

where Z_p denotes the pair of poles of the PMSM. The rotation of motor could be described by the following dynamic equation:

$$J_m \frac{d\omega_m}{dt} = T_e - B_v \omega_m - T_L \tag{1.59}$$

with J_m denoting the total inertia, B_v viscous friction coefficient and T_L load torque. Replacing the mechanical speed (ω_m) with electrical speed ω_e in (1.59) gives

$$\frac{d\omega_e}{dt} = \frac{Z_p}{J_m}\left(T_e - \frac{B_v}{Z_p}\omega_e - T_L\right). \tag{1.60}$$

For the surface mounted PMSM or $i_d = 0$ control, there is no additional torque component. Thus, substituting the torque (1.46) into (1.60) yields

$$\frac{d\omega_e}{dt} = \frac{Z_p}{J_m}\left(\frac{3}{2}Z_p \phi_{mg} i_q - \frac{B_v}{Z_p}\omega_e - T_L\right). \tag{1.61}$$

Together with the electrical model derived in the last section, the complete model of a PMSM is represented by

$$\frac{di_d}{dt} = \frac{1}{L_d}(v_d - R_s i_d + \omega_e L_q i_q) \tag{1.62}$$

$$\frac{di_q}{dt} = \frac{1}{L_q}(v_q - R_s i_q - \omega_e L_d i_d - \omega_e \phi_{mg}) \tag{1.63}$$

$$\frac{d\omega_e}{dt} = \frac{Z_p}{J_m}\left(\frac{3}{2}Z_p \phi_{mg} i_q - \frac{B_v}{Z_p}\omega_e - T_L\right). \tag{1.64}$$

1.4 Per Unit Model and PMSM Parameters

Using the explicit machine model (1.62) to (1.64) with SI unit to design the controller could lead to numerical problems due to different units of machine parameters and variables. For example, in the third equation (1.64), a small inertia value (J_m) in kg $\cdot$ m^2 may lead to a very large coefficient for i_q in Amp. As a result, the controller gain becomes numerically very small for speed control purpose. Such wide variation of numerical ranges makes the implementation on micro-controllers or Digital Signal Processors (DSP) rather complex. Hence it is more convenient to use the per unit model of the PMSM for the design of controllers.

1.4.1 Per Unit Model and Physical Parameters

In the per unit model, as an example, the base values of parameters and variables of a PMSM are listed in Table 1.1. Here, only three independent base values need to be given. With the three independent

Table 1.1 Base values for the per unit model

Symbol	Description	Base value	SI unit
P_b	Rated power	0.35	kW
U_b	Rated voltage	$150/\sqrt{3}$	V
T_b	Rated torque	1.1	Nm
I_b	Current	8.083	A
R_b	Resistance	10.71	Ω
ω_{eb}	Velocity	630.63	rad/s
L_b	Inductance	0.017	H
Φ_b	Flux	0.1373	Wb
J_b	Inertia	0.0018	$kg \cdot m^2$
B_b	Viscous coefficient	0.0018	$Nm \cdot s$

values P_b, U_b and T_b chosen for this case, the other base values can be obtained by their inherent relationships,

$$I_b = Z_p P_b / U_b,\ R_b = U_b / I_b,\ \omega_{eb} = U_b I_b / T_b$$
$$\phi_b = U_b / \omega_{eb},\ L_b = R_b / \omega_{eb}$$
$$J_b = Z_p P_b / \omega_{eb}^2,\ B_b = T_b / \omega_{eb}.$$

Scaling the parameters and variables in (1.62) to (1.64) with their own base values, the per unit version of a machine model is

$$\frac{di_d}{dt} = \frac{\omega_{eb}}{L_d}(v_d - R_s i_d + \omega_e L_q i_q) \tag{1.65}$$

$$\frac{di_q}{dt} = \frac{\omega_{eb}}{L_q}(v_q - R_s i_q - \omega_e L_d i_d - \omega_e \phi_{mg}) \tag{1.66}$$

$$\frac{d\omega_e}{dt} = \frac{Z_p}{J_m}\left(\frac{3}{2} Z_p \phi_{mg} i_q - \frac{B_v}{Z_p}\omega_e - T_L\right), \tag{1.67}$$

where the notation refers to the per unit value of the machine variables and parameters with the exception that ω_{eb} is in SI units. The numerical values and their per unit counterparts of machine parameters used in obtaining the experimental and simulation results in this book are given in Table 1.2.

1.4.2 Experimental Validation of PMSM Model

The physical model developed is to be validated against the experimental data collected from the test-bed that is described in detail in Chapter 10. The PMSM test-bed has its physical parameters defined by Table 1.2. Using the parameters defined in the table, the differential equations (1.62)–(1.64) are solved to yield the responses of i_d, i_q currents and velocity ω_e. In both simulations and experiments, identical step signals are applied to the v_d and v_q voltages as input to the dynamic system. The load torque $T_L = 0$ Nm in both simulation and experimental validation. Figure 1.6 shows the experimental validation results when the direct axis voltage is a step signal with amplitude 5 and v_q is a step signal with amplitude of 20 (V). With these input voltage signals, the steady-state of the currents i_d (see Figure 1.6(a)) reaches

Table 1.2 Parameters of PMSM

Symbol	Description	SI value	SI unit	Per unit
J_m	Total inertia	0.47×10^{-4}	$kg \cdot m^2$	0.0267
B_v	Viscous coeff.	1.1×10^{-4}	$Nm \cdot s$	0.0625
L_d	d-axis inductance	7.0×10^{-3}	H	0.4120
L_q	q-axis inductance	7.0×10^{-3}	H	0.4120
T_L	Load torque	unknown	Nm	unknown
R_s	Resistance	2.98	Ω	0.2781
ϕ_{mg}	Flux linkage due to permanent magnet	0.125	Wb	0.9102
i_{rated}	Nominal current	2.9	A	0.36
Z_p	No. of pole pairs	2		

1.75 A and i_q (see Figure 1.6(b)) reaches zero from the simulation results and the velocity reaches 73 rad/s (see Figure 1.6(c)). The steady-state of the i_q current is zero because the motor is not loaded and the load torque is zero. In comparison between the simulation and experimental results, the physical model developed here has a high fidelity in both transient responses and steady-state responses. The discrepancies between the responses obtained using the model and those from the experimental test-bed could be explained as the result of the net effects of the PWM harmonics (see Chapter 2), measurement noise, pulsing torque, iron saturation and many other factors, which are ignored in the model.

1.5 Modeling of Induction Motor

Induction motor, or in other words, asynchronous motor generally contains two main components in its structure: stator winding and rotor winding. Stator winding is supplied by an *AC* power source, which will generate a rotating magnetic field, the so-called stator flux. Then, the constantly changing flux will cause a current induced in the rotor winding based on Lenz's Law, subsequently this induced current will generate a magnetic field, the so-called rotor flux. Since both fluxes are opposite to each other, a rotational force is generated to accelerate the rotor until the magnetizing torque is balanced to the load torque. Because the actual rotor's position is always lagging the flux position, in order to ensure the flux cutting through the rotor winding, there is a difference between the angular speed ω_s of the magnetic field and the rotor electrical speed ω_e, which is called *slip* with $\omega_{slip} = \omega_s - \omega_e$. ω_s is also called synchronous flux angular speed.

The traditional three-phase *AC* induction motor has two types, wound and squirrel-cage, which describes the form of the rotor winding. The wound rotor form has a brushed external connection; typical applications include the wind-farm generators. The squirrel-cage rotor is more widely applied and it has the rotor winding connection as a short-circuit without any external connections. The induction motor discussed in this book is of the squirrel-cage type.

1.5.1 Space Vector Representation of Voltage Equation of Induction Motor

The use of the space vector simplifies the derivation of voltage equation for the induction machine and makes the model derivation easier to understand. This derivation is the key to forming the dynamic models for current control.

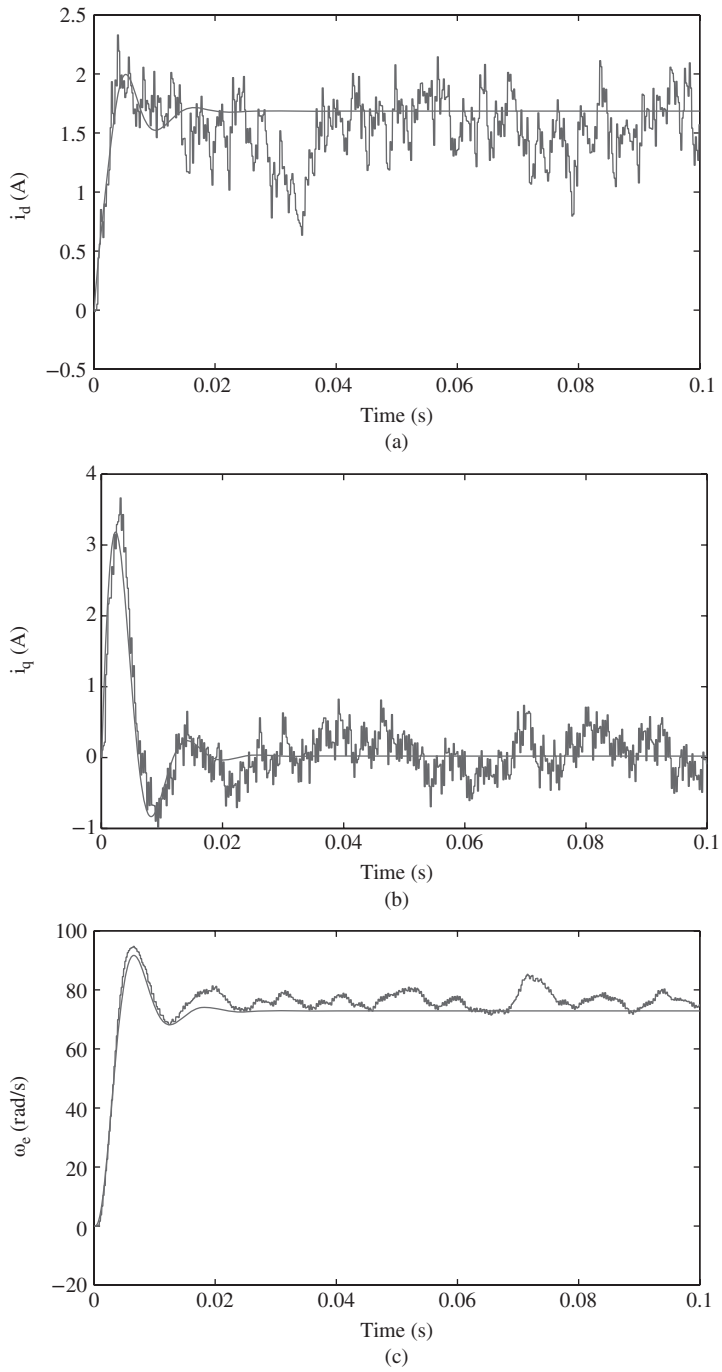

Figure 1.6 Experimental validation (input voltage $v_d = 5$ V and $v_q = 20$ V). Noise free line: model outputs; noisy line: outputs from test-bed. (a) i_d, (b) i_q, and (c) ω_e.

In modeling of the induction motor, the space vector for its three-phase stator current is written as

$$\vec{i_s} = \frac{2}{3}\left(i_a(t) + i_b(t)e^{j\frac{2\pi}{3}} + i_c(t)e^{j\frac{4\pi}{3}s}\right)$$
$$\vec{i_s} = I_s e^{j(\omega_s t+\phi)},$$

where ω_s is the angular speed of the stator side space vectors, and the space vector of three-phase stator voltage is defined as

$$\vec{u_s} = \frac{2}{3}\left(u_a(t) + u_b(t)e^{j\frac{2\pi}{3}} + u_c(t)e^{j\frac{4\pi}{3}}\right),$$

where $u_a(t)$, $u_b(t)$ and $u_c(t)$ are terminal line-to-neutral voltage for each phase, respectively. Similarly, space vectors of three-phase rotor voltage and current are denoted by $\vec{u_r}$ and $\vec{i_r}$. The rotor dynamics play an important role in the mathematical model of an induction motor.

For a squirrel-cage induction motor, the space vector voltage equation of stators with respect to their own winding systems is

$$\vec{u_s} = R_s\vec{i_s} + \frac{d\vec{\psi_s}}{dt}, \tag{1.68}$$

where R_s is the stator resistance and $\vec{\psi_s}$ is the space vector of stator flux. With respect to its own winding system, the space vector voltage equation of the rotor is

$$\vec{u_r}^* = R_r\vec{i_r}^* + \frac{d\vec{\psi_r}^*}{dt} = 0, \tag{1.69}$$

where R_r is the rotor resistance, $\vec{i_r}^*$, $\vec{u_r}^*$ and $\vec{\psi_r}^*$ are rotor's current, voltage and flux in space vector forms with respect to the rotor reference frame. Due to the short-circuit of the rotor winding, the rotor voltage vector in (1.69) is always equal to zero.

In order to synchronize the reference frame of the rotor windings with the reference frame of the stator windings, a set of space vectors are defined to change the reference frame of the space vectors of the rotor,

$$\vec{u_r} = \vec{u_r}^* e^{j\theta_e}$$
$$\vec{i_r} = \vec{i_r}^* e^{j\theta_e}$$
$$\vec{\psi_r} = \vec{\psi_r}^* e^{j\theta_e},$$

where $\theta_e = \omega_e t$, θ_e is the electrical angle of the rotor, and ω_e is the electrical angular speed of the rotor. This transformation is based on the electrical field of the rotor windings lagging behind that of the stator by θ_e radians; thus, in order to synchronize these two reference frames, the space vectors in the rotor reference frame are advanced with the angle θ_e.

Now, multiplying both sides of (1.69) with the factor $e^{j\theta_e}$ and substituting the transformations into the rotor voltage equation leads to

$$\vec{u_r} = R_r\vec{i_r} + \frac{d\vec{\psi_r}}{dt} - j\omega_e\vec{\psi_r} = 0, \tag{1.70}$$

where the following equality is used,

$$\frac{d\vec{\psi_r}}{dt}e^{j\theta_e} = \frac{d\vec{\psi_r}}{dt} - j\omega_e\vec{\psi_r}.$$

With the space vectors of both currents in stator and rotor, the instantaneous fluxes of both windings are given based on their relationships to currents:

$$\vec{\psi_s} = L_s\vec{i_s} + L_h\vec{i_r} \tag{1.71}$$

$$\vec{\psi_r} = L_h\vec{i_s} + L_r\vec{i_r} \tag{1.72}$$

where L_h is the mutual machine inductance, L_s and L_r are the stator and rotor inductance, respectively.

Note that there are coupling terms in the stator flux (see (1.71)) and rotor flux (see (1.72)). It seems that the derivation of the induction motor model is more complicated than the process used in the PMSM model, however, they follow the same thought process. Here it is to eliminate the rotor current $\vec{i_r}$ from the equations and find the relationship between the stator voltage and current.

Taking derivative of stator flux based on (1.71), and substituting the stator flux with stator and rotor currents, the stator voltage equation (1.68) becomes:

$$\vec{u_s} = R_s \vec{i_s} + L_s \frac{d\vec{i_s}}{dt} + L_h \frac{d\vec{i_r}}{dt}. \tag{1.73}$$

To eliminate the rotor current $\vec{i_r}$, the rotor flux equation (1.72) is used to find

$$\vec{i_r} = \frac{1}{L_r}\vec{\psi_r} - \frac{L_h}{L_r}\vec{i_s}.$$

Substituting this into (1.73) yields

$$\vec{u_s} = R_s \vec{i_s} + L_s \left(1 - \frac{L_h^2}{L_s L_r}\right) \frac{d\vec{i_s}}{dt} + \frac{L_h}{L_r} \frac{d\vec{\psi_r}}{dt}.$$

To eliminate the derivative of the rotor flux from the above equation, the voltage balance equation from the rotor (see (1.70)) is used, which leads to

$$\frac{d\vec{\psi_r}}{dt} = -\frac{R_r}{L_r}\vec{\psi_r} + \frac{R_r L_h}{L_r}\vec{i_s} + j\omega_e \vec{\psi_r},$$

where the rotor current is replaced with stator flux and current. Finally, it can be verified that the stator voltage equation is expressed in terms of the rotor flux and stator current:

$$\vec{u_s} = \left(R_s + R_r \frac{L_h^2}{L_r^2}\right)\vec{i_s} + L_s \left(1 - \frac{L_h^2}{L_s L_r}\right) \frac{d\vec{i_s}}{dt} + \left(-\frac{L_h R_r}{L_r^2} + j\omega_e \frac{L_h}{L_r}\right)\vec{\psi_r}.$$

Although all the physical parameters are defined in the above model, they could have more compact expressions. More specifically, define the following parameters used in the model, leakage factor:

$$\sigma = 1 - \frac{L_h^2}{L_s L_r}, \tag{1.74}$$

stator time constant:

$$\tau_s = \frac{L_s}{R_s}, \tag{1.75}$$

rotor time constant:

$$\tau_r = \frac{L_r}{R_r}, \tag{1.76}$$

coefficients:

$$k_r = \frac{L_h}{L_r} \tag{1.77}$$

$$r_\sigma = R_s + R_r k_r^2 \tag{1.78}$$

$$\tau'_\sigma = \frac{\sigma L_s}{r_\sigma}. \tag{1.79}$$

With these definitions of parameters, the voltage equation in space vector form is simply expressed as

$$\vec{i_s} + \tau'_\sigma \frac{d\vec{i_s}}{dt} = \frac{k_r}{r_\sigma}\left(\frac{1}{\tau_r} - j\omega_e\right)\vec{\psi_r} + \frac{1}{r_\sigma}\vec{u_s} \tag{1.80}$$

where the rotor flux satisfies the differential equation:

$$\vec{\psi_r} + \tau_r \frac{d\vec{\psi_r}}{dt} = j\omega_e \tau_r \vec{\psi_r} + L_h \vec{i_s}. \tag{1.81}$$

1.5.2 Representation in Stationary $\alpha - \beta$ Reference Frame

Upon obtaining the electrical model in the space vector form, the next step is to convert it to the model in the $\alpha - \beta$ reference frame. The $\alpha - \beta$ reference frame is a stationary reference frame in the stator side with the real (α) axis aligned with the peak MMF ($F_a(t)$, see Figures 1.1 and 1.3) and the imaginary (β) axis in quadrature (see Figure 1.3).

By decomposing the space vector voltage, current and flux onto the real and imaginary axes, they can be represented by the complex notations,

$$\vec{u_s} = u_{s\alpha} + ju_{s\beta} \tag{1.82}$$

$$\vec{i_s} = i_{s\alpha} + ji_{s\beta} \tag{1.83}$$

$$\vec{\psi_r} = \psi_{r\alpha} + j\psi_{r\beta}. \tag{1.84}$$

To obtain the dynamic model in the $\alpha - \beta$ reference frame, the above variables are substituted into the space vector model (1.80) and (1.81).

It can be readily verified that the electrical model of the induction motor in the $\alpha - \beta$ reference frame is described by the following four differential equations:

$$\frac{di_{s\alpha}}{dt} = -\frac{1}{\tau'_\sigma} i_{s\alpha} + \frac{k_r}{r_\sigma \tau'_\sigma \tau_r}\psi_{r\alpha} + \frac{k_r}{r_\sigma \tau'_\sigma}\omega_e \psi_{r\beta} + \frac{1}{r_\sigma \tau'_\sigma} u_{s\alpha} \tag{1.85}$$

$$\frac{di_{s\beta}}{dt} = -\frac{1}{\tau'_\sigma} i_{s\beta} - \frac{k_r}{r_\sigma \tau'_\sigma}\omega_e \psi_{r\alpha} + \frac{k_r}{r_\sigma \tau'_\sigma \tau_r}\psi_{r\beta} + \frac{1}{r_\sigma \tau'_\sigma} u_{s\beta} \tag{1.86}$$

$$\frac{d\psi_{r\alpha}}{dt} = \frac{L_h}{\tau_r} i_{s\alpha} - \frac{1}{\tau_r}\psi_{r\alpha} - \omega_e \psi_{r\beta} \tag{1.87}$$

$$\frac{d\psi_{r\beta}}{dt} = \frac{L_h}{\tau_r} i_{s\beta} + \omega_e \psi_{r\alpha} - \frac{1}{\tau_r}\psi_{r\beta}. \tag{1.88}$$

1.5.3 Representation in $d - q$ Reference Frame

To change the reference frame to the $d - q$ frame is equivalent to rotating the space vector in $\alpha - \beta$ frame clockwise by θ_s, that is

$$\vec{u_s}' = \vec{u_s} e^{-j\theta_s} = u_{sd} + ju_{sq} \tag{1.89}$$

$$\vec{i_s}' = \vec{i_s} e^{-j\theta_s} = i_{sd} + ji_{sq} \tag{1.90}$$

$$\vec{\psi_r}' = \vec{\psi_r} e^{-j\theta_s} = \psi_{rd} + j\psi_{rq}, \tag{1.91}$$

where $\vec{u}_s'$, $\vec{i}_s'$ and $\vec{\psi}_r'$ denote the space vectors referred to rotating $d-q$ frame. $\theta_s = \omega_s t$ where ω_s is the synchronous flux angular speed in the stator. In this rotating $d-q$ reference frame, the rotor flux vector is fixed to the real axis of the coordinate system. Therefore, the quadrature component of $\vec{\psi}_r'$ is zero.

Multiplying (1.80) with the factor $e^{-j\theta_s}$ and substituting in the space vectors in $d-q$ frame gives

$$\vec{i}_s' + \tau_\sigma' \left(\frac{d\vec{i}_s'}{dt} + j\omega_s \vec{i}_s' \right) = \frac{k_r}{r_\sigma} \left(\frac{1}{\tau_r} - j\omega_e \right) \vec{\psi}_r' + \frac{1}{r_\sigma} \vec{u}_s', \tag{1.92}$$

where the following equality is used:

$$\frac{d\vec{i}_s}{dt} e^{-j\theta_s} = \frac{d\vec{i}_s'}{dt} + j\omega_s \vec{i}_s'.$$

Based on the real and imaginary components of (1.92), the dynamic electrical model in the $d-q$ reference frame is obtained:

$$\frac{di_{sd}}{dt} = -\frac{1}{\tau_\sigma'} i_{sd} + \omega_s i_{sq} + \frac{k_r}{r_\sigma \tau_\sigma' \tau_r} \psi_{rd} + \frac{1}{r_\sigma \tau_\sigma'} u_{sd} \tag{1.93}$$

$$\frac{di_{sq}}{dt} = -\omega_s i_{sd} - \frac{1}{\tau_\sigma'} i_{sq} - \frac{k_r}{r_\sigma \tau_\sigma'} \omega_e \psi_{rd} + \frac{1}{r_\sigma \tau_\sigma'} u_{sq}. \tag{1.94}$$

Similarly, it can be shown that the rotor flux in the $d-q$ reference frame satisfies:

$$\frac{d\psi_{rd}}{dt} = \frac{L_h}{\tau_r} i_{sd} - \frac{1}{\tau_r} \psi_{rd} \tag{1.95}$$

$$0 = \frac{L_h}{\tau_r} i_{sq} - (\omega_s - \omega_e) \psi_{rd}, \tag{1.96}$$

where the q component of rotor flux $\psi_{rq} = 0$. Since Equation (1.96) is an algebraic equation, it is not included for control design. However, it yields the relationship used for estimation of ω_s:

$$\omega_s = \omega_e + \frac{L_h}{\tau_r} \frac{i_{sq}}{\psi_{rd}}, \tag{1.97}$$

which is also called slip estimation and ω_e is the electrical angular velocity of the rotor. Since the rotor flux ψ_{rd} is not directly measured, the slip estimation is alternatively performed using the current i_{sd} to replace ψ_{rd} as

$$\omega_s = \omega_e + \frac{1}{\tau_r} \frac{i_{sq}}{i_{sd}}, \tag{1.98}$$

where $\frac{d\psi_{rd}}{dt} = 0$ is assumed in (1.95) to obtain the steady-state solution of i_{sd} in relation to ψ_{rd}.

Relationships exist between the current, voltage and flux variables in the $\alpha-\beta$ reference frame and the $d-q$ reference frame, governed by the Clarke transformation (see Figure 1.4 for illustration), and they are given below:

$$\begin{bmatrix} u_{sd} \\ u_{sq} \end{bmatrix} = \begin{bmatrix} \cos\theta_s & \sin\theta_s \\ -\sin\theta_s & \cos\theta_s \end{bmatrix} \begin{bmatrix} u_{s\alpha} \\ u_{s\beta} \end{bmatrix} \tag{1.99}$$

$$\begin{bmatrix} i_{sd} \\ i_{sq} \end{bmatrix} = \begin{bmatrix} \cos\theta_s & \sin\theta_s \\ -\sin\theta_s & \cos\theta_s \end{bmatrix} \begin{bmatrix} i_{s\alpha} \\ i_{s\beta} \end{bmatrix} \tag{1.100}$$

$$\begin{bmatrix} \psi_{rd} \\ \psi_{rq} \end{bmatrix} = \begin{bmatrix} \cos\theta_s & \sin\theta_s \\ -\sin\theta_s & \cos\theta_s \end{bmatrix} \begin{bmatrix} \psi_{r\alpha} \\ \psi_{r\beta} \end{bmatrix}. \tag{1.101}$$

1.5.4 Electromagnetic Torque of Induction Motor

The electromagnetic torque of induction motor is calculated using the cross product of the space vectors of rotor flux and and stator current in the $d-q$ reference frame, which is

$$T_e = \frac{3}{2} Z_p \frac{L_h}{L_r} (\vec{\psi}_r' \otimes \vec{i}_s'), \tag{1.102}$$

where Z_p is the number of pole pairs. The cross product, defined in Section 1.2.3, is calculated using two three dimensional vectors $[\psi_{rd} \quad 0 \quad 0]$ and $[i_{sd} \quad i_{sq} \quad 0]$ since ψ_{rq} is zero. The result of the cross product is the vector $[0 \quad 0 \quad \psi_{rd} i_{sq}]$. Thus, in the $d-q$ reference frame, the electromagnetic torque is proportional to $\psi_{rd} i_{sq}$, which is

$$T_e = \frac{3}{2} Z_p \frac{L_h}{L_r} \psi_{rd} i_{sq}. \tag{1.103}$$

If the electromagnetic torque is calculated using the space vectors of rotor and stator current in the $\alpha-\beta$ reference frame, then it is proportional to the cross product of the space vectors of rotor flux and stator current in the stationary frame,

$$\begin{aligned} T_e &= \frac{3}{2} Z_p \frac{L_h}{L_r} (\vec{\psi}_r \otimes \vec{i}_s) \\ &= \frac{3}{2} Z_p \frac{L_h}{L_r} (\psi_{r\alpha} i_{s\beta} - \psi_{r\beta} i_{s\alpha}). \end{aligned} \tag{1.104}$$

Note that the expression of electromagnetic torque T_e in the $d-q$ reference frame is only related to ψ_{rd} and i_{sq}. These two variables are *DC* variables, thus the torque control can be achieved by controlling ψ_{rd} and i_{sq} to their specified constant or piece-wise constant reference signals. On the other hand, in the $\alpha-\beta$ reference frame, it is much more difficult to achieve torque control because the expression in (1.104) is associated with the fluxes in $\alpha-\beta$ reference frame that are sinusoidal signals.

The mechanical model of induction motor is derived from the general motion equation of motor rotation, which is given as follows,

$$J_m \frac{d\omega_m}{dt} + f_d \omega_m = T_e - T_L, \tag{1.105}$$

where $\omega_m(t)$ is the rotor's mechanical velocity ($\omega_m = \frac{\omega_e}{Z_p}$), J_m represents the inertia of the motor, f_d is the friction coefficient, T_e and T_L denote the electromagnetic torque and load torque, respectively. The dynamic model of the mechanical equation is obtained by substituting Equation (1.104) into the motion equation (1.105), giving

$$\frac{d\omega_m}{dt} = -\frac{f_d}{J_m} \omega_m + \frac{3}{2} \frac{Z_p L_h}{L_r J_m} \psi_{rd} i_{sq} - \frac{T_L}{J_m}. \tag{1.106}$$

In terms of rotor's electrical velocity,

$$\frac{d\omega_e}{dt} = -\frac{f_d}{J_m} \omega_e + \frac{3}{2} \frac{Z_p^2 L_h}{L_r J_m} \psi_{rd} i_{sq} - \frac{Z_p T_L}{J_m}. \tag{1.107}$$

1.5.5 Model Parameters of Induction Motor and Model Validation

The induction motor has the characteristics given by the nameplate data (see Table 1.3), and its parameters used in the physical model are given in Table 1.4. These physical parameters are used in this book for simulations and experiments.

Table 1.3 Nameplate of the induction motor

Manufacturer	SEW-EURODRIVE
Type	3-phase Cage
Rated power	0.75 kW
Supply frequency	50 Hz
Number of pole pairs	2
Rated Speed	1435 RPM
Rated stator current	1.75 A
Rated RMS phase voltage	415 V
Connection	*Y* (star connection)

Table 1.4 Motor parameters

$R_s(\Omega)$	$R_r(\Omega)$	L_s(H)	L_r(H)	L_h(H)	$J_m(\text{kg}\cdot\text{m}^2)$	$f_d(\text{Nm}\cdot\text{s})$
11.2	8.3	0.6155	0.6380	0.570	0.00214	0.0041

The induction motor model is validated against the test-bed used in this book (see Chapter 10 for a detailed description of the test-bed). In the $d-q$ reference frame, the responses of stator currents i_{sd}, i_{sq}, rotor flux ψ_{rd} and motor mechanical velocity ω_m are calculated by building an induction motor simulator using the MATLAB/Simulink SimPower Toolbox, followed by entering the physical parameters listed in Table 1.4 into this simulator. Choosing the voltage input signals, u_{sd} and u_{sq}, as step signals with amplitudes of 10 V and 100 V respectively, the simulation results of currents, flux and velocity are shown in Figure 1.7. With the identical conditions as the simulation conditions, experiments are conducted using the test-bed. Figure 1.8 shows the experimental results of the currents, flux and velocity. By comparing these two figures, it is seen that the steady-state responses are very similar; however, the transient responses from the actual motor are faster than those produced by the

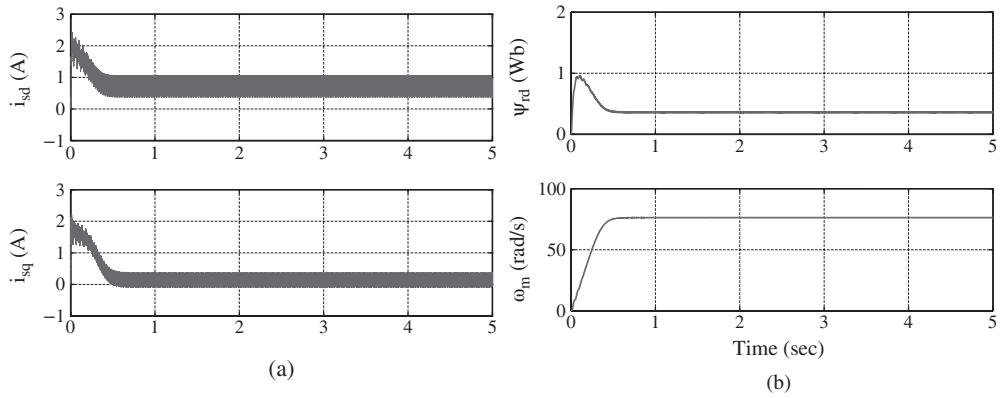

Figure 1.7 Simulation result using SimPower model. (a) i_{sd} and i_{sq} currents and (b) Flux and velocity.

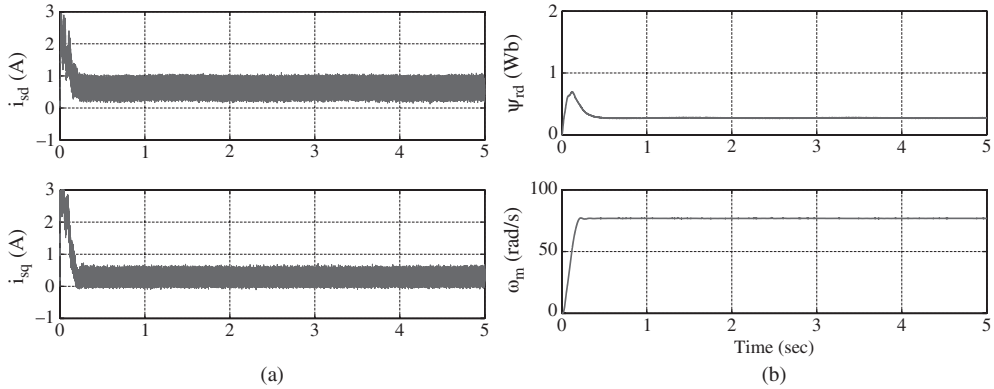

Figure 1.8 Experimental results. (a) i_{sd} and i_{sq} currents and (b) Flux and velocity.

Simulink simulator. Also, due to the PWM mechanisms used in both the simulation and experiment, the stator currents i_{sd} and i_{sq} contain substantial amount of harmonics (see Figures 1.7–1.8), particularly in the steady-state operations. Discussions about harmonics in the *AC* drives can be found in Chapter 2.

For those who are interested in how to build a Simulink simulator using SimPower Toolbox, a step-by-step tutorial for such a practice is given in Chapter 10.

1.6 Modeling of Power Converter

Figure 1.9 shows the block diagram of a grid-connected three phase voltage source converter. The symbols $[S_a, \overline{S_a}], [S_b, \overline{S_b}], [S_c, \overline{S_c}]$ in Figure 1.9 denote six bipolar switching inputs with either value of 0 or 1 for an upper and lower leg of each phase respectively. These switching inputs are conducted in a complementary manner, for example, at any given time $S_a + \overline{S_a} = 1$, $S_b + \overline{S_b} = 1$, $S_c + \overline{S_c} = 1$. This means that only one of the switches is allowed to conduct at any one time.

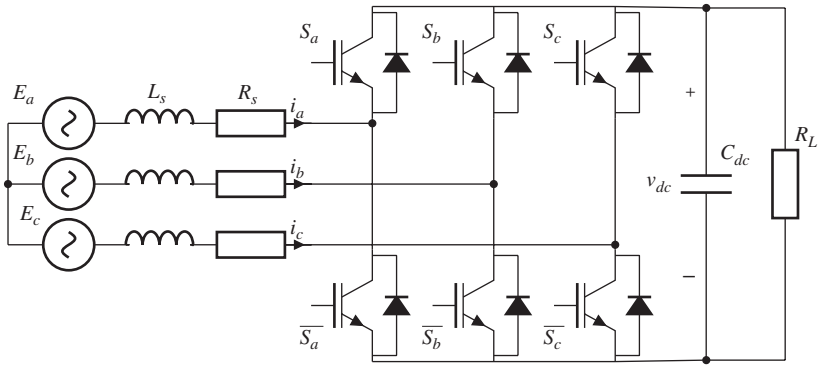

Figure 1.9 Block diagram of two level voltage source converter.

Before proceeding to the model derivation, several assumptions are made about the operation of the converter. Firstly, it is assumed that all switches are ideal and operate in a continuous conduction mode (CCM), and the grid voltage is symmetric and balanced as follows.

$$E_a = E_m \cos(\omega_g t) \tag{1.108}$$

$$E_b = E_m \cos\left(\omega_g t - \frac{2\pi}{3}\right) \tag{1.109}$$

$$E_c = E_m \cos\left(\omega_g t - \frac{4\pi}{3}\right), \tag{1.110}$$

where $\omega_g = 2\pi f$, f is the grid frequency (50 Hz used in this book). Secondly, the system is assumed to be a three wire system, thus the sum of three phase currents and voltage is equal to zero.

$$i_a + i_b + i_c = 0 \tag{1.111}$$

$$E_{an} + E_{bn} + E_{cn} = 0. \tag{1.112}$$

Thirdly, it is assumed that the inductance and resistance parameters, L_s and R_s, are ideal, therefore, they have the same values for the three phase system. Even though these assumptions are ideal and do not hold entirely in applications, their acceptance ensures the derivation of the dynamic model in a simpler manner.

1.6.1 Space Vector Representation of Voltage Equation for Power Converter

The use of space vector simplifies the derivation of voltage equation for the two level voltage source power converter. The space vector for three-phase grid current can be written as

$$\vec{i_s} = \frac{2}{3}\left(i_a(t) + i_b(t)e^{j\frac{2\pi}{3}} + i_c(t)e^{j\frac{4\pi}{3}}\right), \tag{1.113}$$

while the space vector of three-phase voltage at the three nodes, on the grid side linked with the converter, is defined as

$$\vec{v_s} = \frac{2}{3}\left(v_a(t) + v_b(t)e^{j\frac{2\pi}{3}} + v_c(t)e^{j\frac{4\pi}{3}}\right) \tag{1.114}$$

and the space vector of the three phase grid voltage is described by

$$\vec{E_s} = \frac{2}{3}\left(E_a(t) + E_b(t)e^{j\frac{2\pi}{3}} + E_c(t)e^{j\frac{4\pi}{3}}\right). \tag{1.115}$$

Based on these definitions, the space vector voltage at the nodes of the converter satisfies the voltage equation:

$$\vec{v_s} = -L_s\frac{d\vec{i_s}}{dt} - R_s\overrightarrow{i_s(t)} + \vec{E_s}. \tag{1.116}$$

It is emphasized here that the above space vector voltage equation is obtained at the grid side.

1.6.2 Representation in $\alpha - \beta$ Reference Frame

The next step in the derivation of the model is to convert the model in the space vector form to the model in the $\alpha - \beta$ reference frame. By representing the space vectors, voltage and current, in terms of their real and imaginary components, they can be written in the complex notation,

$$\vec{v_s} = v_\alpha + jv_\beta$$

$$\vec{i_s} = i_\alpha + ji_\beta$$
$$\vec{E_s} = E_\alpha + jE_\beta.$$

To obtain the dynamic model in the $\alpha - \beta$ reference frame, the above variables are substituted into the space vector model (1.116) where the rotating frame in the $\alpha - \beta$ has the same velocity as the rotating speed of the space vector in the grid. Thus, by simply taking the components in the real and imaginary axes, in the $\alpha - \beta$ reference frame, the electrical model of the voltage source converter is described by the following two differential equations:

$$v_\alpha(t) = -L_s \frac{di_\alpha(t)}{dt} - R_s i_\alpha(t) + E_\alpha(t) \tag{1.117}$$

$$v_\beta(t) = -L_s \frac{di_\beta(t)}{dt} - R_s i_\beta(t) + E_\beta(t). \tag{1.118}$$

1.6.3 Representation in $d - q$ Reference Frame

To change the reference frame to the $d - q$ frame is equivalent to rotating the space vectors in (1.116) clockwise by θ_g so that the synchronous reference frame is aligned with the grid voltage at ω_g frequency, where $\theta_g = \omega_g t$ and $\omega_g = 2\pi f$ rad/s, f is the grid frequency in Hz. Thus, the following rotated space vectors are defined:

$$\vec{v_s}' = \vec{v_s} e^{-j\theta_g} = v_d + jv_q \tag{1.119}$$

$$\vec{i_s}' = \vec{i_s} e^{-j\theta_g} = i_d + ji_q \tag{1.120}$$

$$\vec{E_s}' = \vec{E_s} e^{-j\theta_g} = E_d + jE_q, \tag{1.121}$$

where $\vec{v_s}'$, $\vec{i_s}'$ and $\vec{E_s}'$ denote the space vectors referred to rotating $d - q$ frame. The grid voltage in the q-axis, E_q, is zero.

Multiplying (1.116) with the factor $e^{-j\theta_g}$ and replacing the original space vectors by the space vectors ((1.119)–(1.121)) in the rotating frame gives

$$\vec{v_s}' = -L_s \frac{d\vec{i_s}'}{dt} - j\omega_g L_s \vec{i_s}' - R_s \vec{i_s}' + \vec{E_s}', \tag{1.122}$$

where the following equality is used:

$$\frac{d\vec{i_s}}{dt} e^{-j\theta_g} = \frac{d\vec{i_s}'}{dt} + j\omega_g \vec{i_s}'.$$

Based on the real and imaginary components of (1.122), it can be verified that the dynamic model in the $d - q$ reference frame is:

$$v_d = -L_s \frac{di_d(t)}{dt} + \omega_g L_s i_q - R_s i_d + E_d \tag{1.123}$$

$$v_q = -L_s \frac{di_q(t)}{dt} - \omega_g L_s i_d - R_s i_q, \tag{1.124}$$

where $E_q = 0$.

1.6.4 Energy Balance Equation

The output of the voltage source converter is its *DC* voltage v_{dc} on the capacitor (see Figure 1.9). To derive the dynamic model for the v_{dc}, the energy conservation is investigated, where

$$P_c = P_g - P_L.$$

Here, P_c is the power consumed by the capacitor, P_g is power from the grid and P_L is the power consumed by the load. Assuming that the *DC* current for the capacitor is $i_c(t)$, then from the energy conservation, the following equality is obtained:

$$v_{dc} i_c = \frac{3}{2}\vec{v_s} \cdot \vec{i_s} - i_L v_{dc}, \tag{1.125}$$

where $\vec{v_s} \cdot \vec{i_s}$ is the inner product[2] of the space vectors of voltage and current, i_L is the load current. In this equation, the term $v_{dc} i_c$ is the energy conserved in the capacitor, the term $i_L v_{dc}$ is the energy consumption of the load, and the term $\frac{3}{2}\vec{v_s} \cdot \vec{i_s}$ is the energy drawn from the grid, consisting of active power and reactive power.

Since in the $\alpha - \beta$ reference frame, the following relationships hold:

$$\vec{v_s} = v_\alpha + j v_\beta$$
$$\vec{i_s} = i_\alpha + j i_\beta.$$

By substituting these equations into (1.125) and calculating the inner product, the capacitor current satisfies:

$$i_c = \frac{3}{2v_{dc}}(v_\alpha i_\alpha + v_\beta i_\beta) - i_L.$$

Since $i_c = C_{dc}\frac{dv_{dc}}{dt}$, the capacitor voltage v_{dc} is described by the dynamic equation in the $\alpha - \beta$ reference frame:

$$C_{dc}\frac{dv_{dc}}{dt} = \frac{3}{2v_{dc}}(v_\alpha i_\alpha + v_\beta i_\beta) - i_L, \tag{1.126}$$

where C_{dc} is the capacitance.

Similarly, in the $d - q$ reference frame, (1.125) is expressed in terms of the space vectors of current and voltage $\vec{i_s}'$ and $\vec{v_s}'$, which has the form:

$$\begin{aligned} v_{dc} i_c &= \frac{3}{2}\vec{v_s}' \cdot \vec{i_s}' - i_L v_{dc} \\ &= \frac{3}{2}(v_d i_d + v_q i_q) - i_L v_{dc}, \end{aligned} \tag{1.127}$$

leading to the capacitor voltage v_{dc} described in the $d - q$ reference frame as

$$C_{dc}\frac{dv_{dc}}{dt} = \frac{3}{2v_{dc}}(v_d i_d + v_q i_q) - i_L. \tag{1.128}$$

Supposing that at steady state operating conditions, the converter maintains a target *DC* bus voltage with unity power factor, the reference signal to the i_q current is chosen to be zero in order to achieve this control objective.

[2] The inner product of two vectors $\vec{a}$ and $\vec{b}$ is the scalar $c = \vec{a} \cdot \vec{b}$. Letting $\vec{a} = [a_1, a_2]$ and $\vec{b} = [b_1, b_2]$, the scalar $c = a_1 b_1 + a_2 b_2$ (see Kreyszig (2010)).

1.7 Summary

This chapter has derived the physical models of PMSM, induction machine and voltage source power converter in both stationary reference frame (also called $\alpha - \beta$ reference frame) and synchronous reference frame (also called $d - q$) reference frame.

There are two steps deployed in the derivation of the mathematical models. The first step is to use space vector description of the physical variables for voltage, current and flux, and the second step is to convert the space vector based model to various reference frames. The mathematical models are presented in terms of differential equations that will be used for control system design in the future chapters.

1.8 Further Reading

General application characteristics of electric motors are discussed in Pillay and Krishnan (1991). Books for electrical drives include Vas (1992), Vas (1993) Hughes and Drury (2013), Leonhard (2001), El-Hawary (2011), Drury (2009), Quang and Dittrich (2008), Linder *et al.* (2010). Modeling and simulation of *AC* motor drive was discussed in Pillay and Krishnan (1988), Pillay and Krishnan (1989), Holtz (1994), Filho and de Souza (1997), Lorenz *et al.* (1994) and Ong (1998). Mathematical modeling and analysis of converters were presented in Wu *et al.* (1991), in Lindgren (1998), in Abdel-Rahim and Quaicoe (1994), in Blasko and Kaura (1997). The Park transformation was described in Park (1929) and the Clarke transformation was described in Duesterhoeft *et al*. (1951). A system theory approach to unify electrical machine analysis was discussed in Willems (1972).

References

Abdel-Rahim N and Quaicoe JE 1994 Modeling and analysis of a feedback control strategy for three- phase voltage-source utility interface systems. *Proceedings of the 29th IAS Annual Meeting* pp. 895–902.

Blasko V and Kaura V 1997 A new mathematical model and control of a three-phase AC-DC voltage source converter. *IEEE Transations on Power Electronics*.

Drury B 2009 *The Control Techniques drives and controls handbook* 2nd edn. IET.

Duesterhoeft W, Schulz MW and Clarke E 1951 Determination of instantaneous currents and voltages by means of alpha, beta, and zero components. *Transactions of the American Institute of Electrical Engineers* **70**(2), 1248–1255.

El-Hawary M 2011 *Principles of Electric Machines with Power Electronic Applications* 2nd edn. IEEE Press.

Filho E and de Souza R 1997 Three-phase induction motor dynamic mathematical model *IEEE International Electric Machines and Drives Conference Record*, pp. MB1/2.1 – MB1/2.3.

Holtz J 1994 The induction motor-a dynamic system *20th International Conference on Industrial Electronics, Control and Instrumentation*, vol. 1, p. P1.

Hughes A and Drury B 2013 *Electric Motors and Drives: Fundamentals, Types and Applications* 4th edn. Elsevier.

Kreyszig E 2010 *Advanced Engineering Mathematics* 10th edn. John Wiley and Sons, New York.

Leonhard W 2001 *Control of Electrical Drives* 3rd edn. Springer.

Linder A, Kanchan R, Kennel R and Stolze P 2010 *Model-Based Predictive Control of Electric Drives*. Cuvillier.

Lindgren M 1998 *Modeling and control of voltage source converters connected to the grid* PhD thesis Chalmers University of Technology.

Lorenz RD, Lipo TA and Novotny DW 1994 Motion control with induction motors. *Proceedings of the IEEE* **82**(8), 1215–1240.

Ong CM 1998 *Dynamic Simulation of Electric Machinery Using MATLAB*. Prentice Hall.

Park RH 1929 Two-reaction theory of synchrobous machines- part I. *AIEE Transations* **48**(2), 716–739.

Pillay P and Krishnan R 1988 Modeling of permanent magnet motor drives. *IEEE Transactions on Industrial Electronics* **35**(4), 537–541.

Pillay P and Krishnan R 1989 Modeling, simulation, and analysis of permanent-magnet motor drives. I. the permanent-magnet synchronous motor drive. *IEEE Transactions on Industry Applications* **25**(2), 265–273.

Pillay P and Krishnan R 1991 Application characteristics of permanent magnet synchronous and brushless DC motors for servo drives. *IEEE Transactions on Industry Applications* **27**(5), 986–996.

Quang NP and Dittrich JA 2008 *Vector Control of Three-Phase AC Machines* 1st edn. Springer.

Vas P 1992 *Electrical Machines and Drives- A Space-Vector Theory Approach*. Oxford University Press, New York, USA.

Vas P 1993 *Parameter Estimation, Condition Monitoring, and Diagnosis of Electrical Machines*. Oxford University Press, New York, USA.

Willems JL 1972 A system theory approach to unified electrical machine analysis. *International Journal of Control* **15**, 401–418.

Wu R, Dewan S and Slemon G 1991 Analysis of an AC-to-DC voltage source converter using PWM with phase and amplitude control. *IEEE Transactions on Industry Applications* **27**(2), 355–364.